Singularities and Poincaré Indices of Electromagnetic Multipoles

Weijin Chen,[1] Yuntian Chen,[1,3,*] and Wei Liu[2,†]
[1]*School of Optical and Electronic Information, Huazhong University of Science and Technology, Wuhan, Hubei 430074, People's Republic of China*
[2]*College for Advanced Interdisciplinary Studies, National University of Defense Technology, Changsha, Hunan 410073, People's Republic of China*
[3]*Wuhan National Laboratory for Optoelectronics, Huazhong University of Science and Technology, Wuhan, Hubei 430074, People's Republic of China*

(Received 22 January 2019; published 19 April 2019)

Electromagnetic multipoles have been broadly adopted as a fundamental language throughout photonics, of which general features such as radiation patterns and polarization distributions are generically known, while their singularities and topological properties have mostly been left unattended. Here we map all the singularities of multipolar radiations of different orders, identify their indices, and show explicitly that the index sum over the entire momentum sphere is always 2, consistent with the Poincaré-Hopf theorem. Upon those revealed properties, we attribute the formation of bound states in the continuum to the overlapping of multipolar singularities with open radiation channels. This insight unveils a subtle equivalence between indices of multipolar singularities and topological charges of those bound states. Our work has fused two fundamental and sweeping concepts of multipoles and topologies, which can potentially bring unforeseen opportunities for many multipole-related fields within and beyond photonics.

DOI: 10.1103/PhysRevLett.122.153907

Electromagnetic multipoles characterized by vector spherical harmonics constitute a complete basis for light field expansions and are playing indispensable roles in diverse branches of optics and photonics [1–3]. Those multipoles have been extensively studied and their general features, such as radiation patterns, polarization distributions, far-field parities, and so on, have been comprehensively exploited for various applications. A rather outstanding example of this is the burgeoning field of metaoptics largely built on electric and magnetic multipoles of different orders, the interferences among which can render enormous extra freedom for manipulating light-matter interactions in both linear and nonlinear regimes [4–7].

In spite of the great achievements relying on electromagnetic multipoles, an unfortunate situation is that rare attention has been paid to those *dark directions* along which there are no radiations. Those directions are naturally considered to be trivial; singularities and topological features of multipoles have neither attracted much interest nor been properly investigated. This is rather puzzling, because from a mathematical viewpoint, in the far field multipolar radiation is transverse and perfectly makes an elementary case of tangent vector fields on a momentum sphere. Depending on the order of multipoles, there are a finite number (at least one) of singularities (zeros or dislocations) of the pure (real or imaginary) vector fields. They are isolated directions where there are no radiations and for which Poincaré indices (winding numbers or topological invariants) can be assigned. Moreover, the Poincaré-Hopf theorem, or more precisely the hairy ball theorem for this specific case, can be simply applied [8–11]. It is even more stunning that such a situation has been stagnant, withstanding the recent overwhelming trend of incorporating topological concepts into almost every branch of physics [12–17]. Considering that electromagnetic multipoles broadly serve as a basic language for descriptions and explanations of various optical effects, to clarify their topological features is of apparently great significance, especially for the expanding field of topological photonics [16,17].

In this Letter, we reapproach electromagnetic multipoles from a topological perspective, focusing on distributions of singularities and their indices of the corresponding tangent vector fields on an S^2 momentum sphere. A comprehensive map is given, pinpointing all singularities with their indices for multipoles of different orders. It is shown explicitly that of all multipoles the index sum over the entire momentum sphere is always 2 (Euler characteristic of a sphere), consistent with the Poincaré-Hopf theorem [8,9]. Based on this revelation, we reinterpret the recently observed bound states in the continuum (BICs) [18] from a multipolar perspective and reveal the origin of overlapping radiation singularities with open radiation channels. We further discover that topological charges of the BICs demonstrated have a multipolar underlying structure, which is essentially equivalent to singularity indices of corresponding multipolar radiations. The incorporation of topological terminology into classical multipoles can potentially rejuvenate many multipole-related studies,

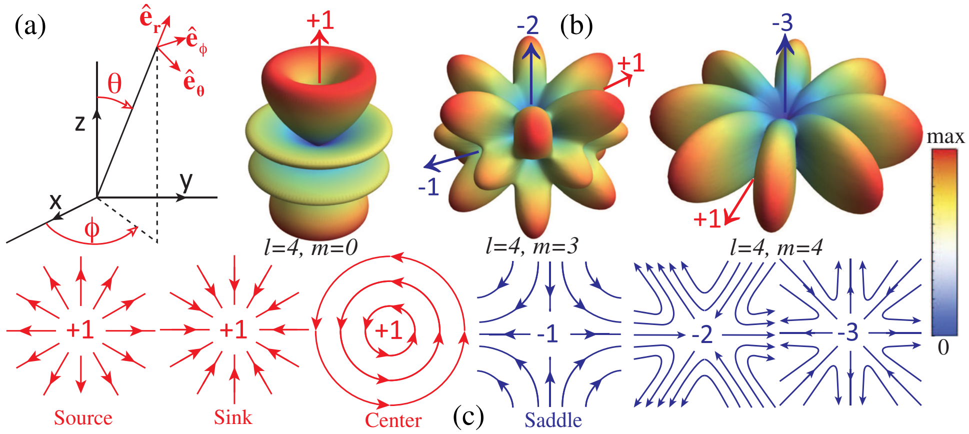

FIG. 1. (a) Spherical polar coordinate system (r, θ, ϕ) with the associated orthonormal basis vectors $\hat{\mathbf{e}}_\theta$, $\hat{\mathbf{e}}_\phi$ and $\hat{\mathbf{e}}_r$ indicated. (b) Radiation patterns for multipoles of order (l, m). Singularities that represent each category of Table I are pinpointed and the corresponding indices are specified. (c) Vector field patterns close to singularities of different indices from -3 to $+1$, which have covered all sorts of singularities indicated in (b).

paving the way for introducing established topological concepts and advanced functionalities into more disciplines both within and beyond photonics [10,11].

Electromagnetic multipoles can be categorized into magnetic and electric groups, the radiated electric (magnetic) fields of which are characterized by vector spherical harmonics $\mathbf{M}_{lm}$ ($\mathbf{N}_{lm}$) and $\mathbf{N}_{lm}$ ($\mathbf{M}_{lm}$), respectively [1,2,19]. For analysis convenience, one specific expression of $\mathbf{M}_{lm}$ is chosen [2,19]

$$\mathbf{M}_{lm} = -\frac{m}{\sin\theta}\sin(m\phi)P_l^m(\cos\theta)\hat{\mathbf{e}}_\theta - \cos(m\phi)\frac{dP_l^m(\cos\theta)}{d\theta}\hat{\mathbf{e}}_\phi. \quad (1)$$

Here we have dropped the radially dependent terms to focus on the tangent fields; $P_l^m(\cos\theta)$ $(-l \leq m \leq l)$ denotes associated Legendre polynomials [23]; basis vectors $\hat{\mathbf{e}}_\theta$, $\hat{\mathbf{e}}_\phi$, and $\hat{\mathbf{e}}_r$, polar and azimuthal angles θ and ϕ are shown in Fig. 1(a); $\mathbf{M}_{lm} \cdot \hat{\mathbf{e}}_\mathbf{r} = 0$ and $\mathbf{N}_{lm} \cdot \mathbf{M}_{lm} = 0$. As a first step, we investigate the poles with $|\cos\theta| = 1$, where ϕ is not defined. Except for $|m| = 1$, both are singularities and the index is as follows [19]:

$$\mathbf{Ind} = 1 - |m|, \qquad |\cos\theta| = 1. \quad (2)$$

When $m = \pm 1$, the poles are not singular, for which we can still assign the index of 0 and thus Eq. (2) is still valid [19].

Next we turn to regions excluding the poles, where for $m = 0$ there are no (isolated) singularities [19]. When $m \neq 0$, according to Eq. (1), a singularity requires that both components along $\hat{\mathbf{e}}_\theta$ and $\hat{\mathbf{e}}_\phi$ are zero, and thus indices and positions of singularities are [19] as follows:

$$\mathbf{Ind} = -1, \qquad \cos(m\phi) = P_l^m(\cos\theta) = 0,$$
$$\mathbf{Ind} = +1, \qquad \sin(m\phi) = \frac{dP_l^m(\cos\theta)}{d\theta} = 0. \quad (3)$$

For $0 < \theta < \pi$ and $0 \leq \phi \leq 2\pi$, both $\sin(m\phi) = 0$ and $\cos(m\phi) = 0$ have $2|m|$ solutions, whereas equations of $P_l^m(\cos\theta) = 0$ and $[dP_l^m(\cos\theta)/d\theta] = 0$ have $l - |m|$ and $l - |m| + 1$ solutions, respectively [23]. It means that except for the poles, there are $2|m|(l - |m|)$ singularities with index of -1 and $2|m|(l - |m| + 1)$ singularities with index of $+1$ (this is still a valid statement for $m = 0$ [19]). Basically the index sum for all singularities is $2(1 - |m|) + 2|m|(l - |m| + 1) - 2|m|(l - |m|)$, which would always make up to 2 and agrees with the Poincaré-Hopf theorem [8,9].

Up to now, we have discussed only magnetic multipoles characterized by $\mathbf{M}_{lm}$ with one specific expression shown in Eq. (1). For the other expression of $\mathbf{M}_{lm}$ [with $\sin(m\phi)$ and $\cos(m\phi)$ interchanged and $\hat{\mathbf{e}}_\theta$ changed to $-\hat{\mathbf{e}}_\theta$ [2,19]), identical distribution map for singularities and indices would be obtained except for an interchange between $\sin(m\phi)$ and $\cos(m\phi)$ in Eq. (3). For electric multipoles characterized by $\mathbf{N}_{lm}$, the duality of Maxwell equations requires that the corresponding tangent fields can be obtained directly from those of $\mathbf{M}_{lm}$ (the terms with radial dependence are dropped for studies of tangent fields) by the following transformation [2,19]: $\hat{\mathbf{e}}_\theta \to \hat{\mathbf{e}}_\phi$ and $\hat{\mathbf{e}}_\phi \to -\hat{\mathbf{e}}_\theta$. Because the transformation above would neither change the position nor the index of the singularity [19], as a result both electric and magnetic multipoles of the same order (l, m) share the same singularity and index distributions, as summarized in Table I. For example, Fig. 1(b) shows radiation patterns and pinpoint some representative singularities with indices for three multipoles (see Ref. [19] for more scenarios). The vector field patterns close to singularities of different indices are shown in Fig. 1(c). For the

TABLE I. Distributions of the singularities and their indices for radiated vector fields from a multipole of order (l, m).

Positions	Index	Number	Total indices
$\lvert\cos(\theta)\rvert = 1$	$1 - \lvert m\rvert$	2	$2(1 - \lvert m\rvert)$
$\cos(m\phi) = P_l^m(\cos\theta) = 0, \lvert\cos(\theta)\rvert \neq 1$	$-1\ (m \neq 0)$	$2\lvert m\rvert \times (l - \lvert m\rvert)$	$-2\lvert m\rvert \times (l - \lvert m\rvert)$
$\sin(m\phi) = [dP_l^m(\cos\theta)/d\theta] = 0, \lvert\cos(\theta)\rvert \neq 1$	$0\ (m = 0)$ $+1\ (m \neq 0)$	$2\lvert m\rvert(l - \lvert m\rvert + 1)$	$2\lvert m\rvert \times (l - \lvert m\rvert + 1)$

case of index $+1$, the singular point could be a source (sink) or a center, depending on which field (electric or magnetic) we employ to show the field lines [19].

Table I shows that a singularity with index larger than $+1$ is not accessible with an individual multipole. In contrast, if a series of multipoles of different orders and/or natures are combined together, a singularity with larger positive index is always accessible, which can be simply justified by the following arguments: for a specific index, we can always predesign a continuous tangent vector field that includes such a singularity; the electromagnetic multipoles constitute an orthogonal and complete bases for vector field expansion; the predesigned vector field can always be expanded into a set of multipoles, with expansion coefficients of a_{lm} and b_{lm} that are associated with $\mathbf{N}_{lm}$ and $\mathbf{M}_{lm}$, respectively [19].

According to the Poincaré-Hopf theorem [8,9], the index sum for all singularities over the momentum sphere should always be 2, being the radiations from an isolated multipole or a set of multipoles. The simplest allowed case of this theorem is that there is only one singularity (at least one singularity) and the index thus has to be $+2$. This corresponds to (generalized) Kerker conditions (Kerker multipoles) or (generalized) Huygens sources [4,5,7]. The field pattern close to a singularity of index $+2$ (also termed as dipole singularity [8,9]) is shown in Fig. 2(a). This type

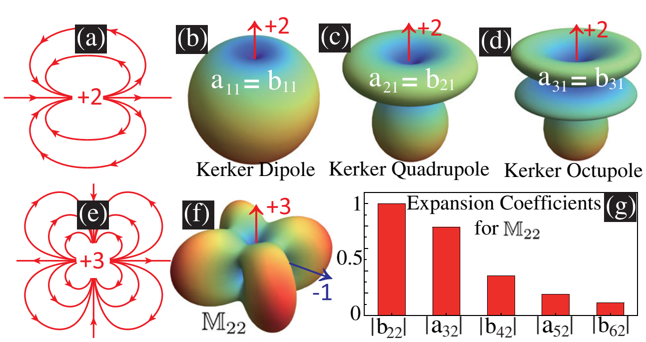

FIG. 2. (a),(e): Vector field patterns close to singularities of indices $+2$ and $+3$. (b)–(d) Multipolar combinations (Kerker dipole, quadrupole, and octupole) that end up with only one singularity of index $+2$. (f) Radiation patterns and singularity distributions for transformed $\mathbb{M}_{22}$, which has to be expanded into a series of multipoles, with normalized magnitudes of expansion coefficients (up to $l = 6$) shown in (g).

of singularity can be obtained from interferences of a pair of electric and magnetic multipoles of the same order, magnitude, and phase ($a_{lm} = b_{lm}$, $m = \pm 1$), but opposite parities [24,25], with the first three cases of overlapping dipoles, quadrupoles, and octupoles shown in Figs. 2(b)–2(d).

For a tangent and continuous vector field $\mathbb{M}_{lm}$ obtained from Eq. (1) by forcing the following transformation (forbidden for $m = \pm 1$ that breaks the continuity of the vector field [19]) $\hat{\mathbf{e}}_\theta \to -\hat{\mathbf{e}}_\theta$ (or equivalently $\hat{\mathbf{e}}_\phi \to -\hat{\mathbf{e}}_\phi$)

$$\mathbb{M}_{lm} = \frac{m}{\sin\theta}\sin(m\phi)P_l^m(\cos\theta)\hat{\mathbf{e}}_\theta - \cos(m\phi)\frac{dP_l^m(\cos\theta)}{d\theta}\hat{\mathbf{e}}_\phi. \tag{4}$$

The singularity distribution table for $\mathbb{M}_{lm}(|m| \neq 1)$ would be the same as Table I, except that the index in the second column is changed from $1 - |m|$, -1, $+1$ to $1 + |m|$, $+1$, -1 [19]. This means that for such a transformed vector field, the index for both singularities at poles would be $1 + |m|$. For example, in Fig. 2(e), we show the field patterns close to a singularity of index $+3$, which is present on the poles of the radiation pattern of $\mathbb{M}_{22}$ [shown in Fig. 2(f); despite the index difference, the radiation pattern is the same as that of $\mathbf{M}_{22}$ [19]]. As has been already explained, $\mathbb{M}_{22}$ cannot be represented by an individual multipole, but by a series of multipoles, with the multipolar composition (normalized magnitudes of expansion coefficients) shown in Fig. 2(g).

After mapping out the singularities and their indices for electromagnetic multipoles, now we proceed to show how those properties could be exploited to gain deeper insights, taking recently demonstrated BICs as an example [18]. For convenience of multipolar analysis, the periodic structure can be approached from an alternative reductionist perspective [26–30]: it can be treated as an infinite ensemble of radiating items (unit cells); the overall optical properties of the periodic structure can be interpreted as interferences of radiations from all the unit cells. For an isolated radiating item, there are an infinite number of open out-coupling radiation channels, corresponding to all the points (directions) on the momentum sphere. In contrast, for the periodic structure, there are only a finite number of such channels, corresponding to diffractions channels of different orders along certain directions. From this perspective, the formation of a BIC can be attributed to overlapping of the radiation singularities of each unit cell with the open diffraction channels of the periodic structure. An index could be assigned to the singularity of the unit-cell radiation that overlaps with the open channel (there can be extra singularities not overlapping with such channels), which is exactly the topological charge of the induced BIC [18,31].

To further crystallize what has been stated above, we turn to the photonic crystal slabs of square or hexagonal lattices,

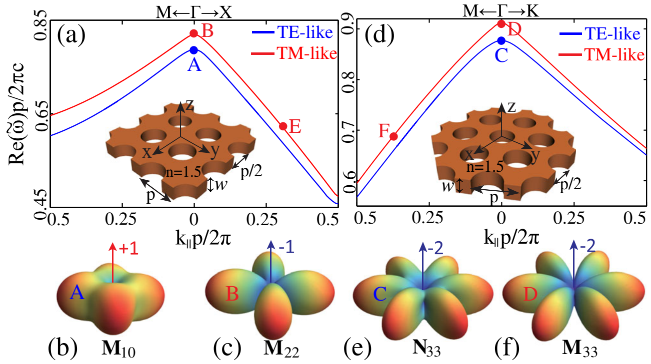

FIG. 3. (a),(d): Dispersion curves for square and hexagonal photonic crystal slabs and six BICs are indicated by points **A–F**: $k_\parallel = \sqrt{k_x^2 + k_y^2}$ is on-plane angular wave number and c is the speed of light. The corresponding radiation patterns and the dominant multipolar components of the four Γ-point BICs are shown in (b),(c) and (e),(f).

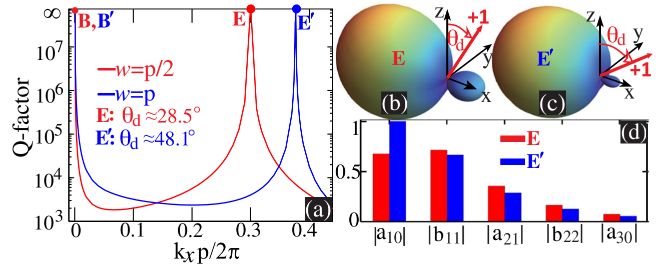

FIG. 4. (a) With width w changed from $p/2$ to p, the off-Γ-point BIC is shifted, whereas the Γ-point BIC is fixed. The multipolar compositions for the two off-Γ-point BICs are shown in (d) (only the major contributing terms are included), and the reconstructed far-field radiation patterns are shown in (b),(c). For both cases, the singularities are of index +1 and overlap with the open diffraction channels.

which are widely employed for investigations into BICs [18,31–36]. For a direct comparison between our results from multipolar analysis with those established ones, and to connect the singularity indices of multipolar radiations to the confirmed topological charges of BICs, we investigate structures similar to those studied in Refs. [31,33]. The photonic crystal slabs of square or hexagonal lattices of circular air holes (slab refractive index $n = 1.5$, width w, lattice constant p, air hole diameter $p/2$) are studied, which are shown as insets in Figs. 3(a) and 3(d). For both cases, we show the dispersion curves of two representative bands (one TE-like and one TM-like bands; $\tilde{\omega}$ is the complex mode eigenfrequency [19]).

First, we check the symmetry-protected BICs located on the Γ points. For both lattices, there are two such BICs on both the TE-like and TM-like bands [four BIC points **A–D** are indicated in Figs. 3(a) and 3(d), with $w = p/2$]. For each of them, we show in Figs. 3(b), 3(c), 3(e), and 3(f) the corresponding major dominant multipolar components (see Ref. [19] for details of multipolar expansions based on near-field currents) and the far-field radiation patters. The four symmetry-protected BICs have a common feature that unit-cell radiation corresponds to that of a dominant individual multipole with fixed order, and the radiation singularity overlaps with the allowed radiation channel (radiation is zero along **z** direction). This agrees with our previous discussions with regard to the multipolar interpretation of the underlying mechanism of BICs. Moreover, based on the dominant multipolar components, for each singularity along **z** direction an index can be directly assigned according to the $|\cos(\theta)| = 1$ category in Table I (other minor multipoles not shown slightly modify the overall radiation pattern, while not affecting singularity and index distributions [19]), which is exactly the topological charge revealed in Ref. [31].

Now we turn to the off-Γ-point accidental BICs [31,33], taking the indicated point **E** ($k_x p/2\pi = 0.299$) in Fig. 3(a) on the TM-like band for example (see similar analysis in Ref. [19] for indicated BIC point **F** in Fig. 3(d) of the hexagonal lattice). We show respectively both its multipolar composition and reconstructed far-field patterns of the unit cell in Figs. 4(b) and 4(d). As expected, Fig. 4(b) shows that a pair of singularities (both of index +1 guaranteed by σ_z mirror symmetry) overlaps with the allowed diffraction directions [$\phi_d = 0$ and $\theta_d = \arcsin(k_x/k_0)$, where k_0 is total the angular wave number]. Moreover, the index +1 of the singularity agrees with the topological charge previously revealed [31]. This BIC would move to another position **E**′ ($k_x p/2\pi = 0.377$) by changing w, as is shown in Fig. 4(a). It is clear from Figs. 4(c) and 4(d) that the multipolar composition changes accordingly such that the multipolar singularity pair coincides with the new diffraction direction, which ensures that the BIC can move smoothly to the new position of different k_x (see Ref. [19] for decay states which correspond to separated singularities and open channels).

Also according to Fig. 4(a), the symmetry-protected BIC is fixed at Γ point with changing w, which can certainly be explained through symmetry analysis [31,35–37]. Our multipolar interpretation gives a different insight: for this type of BIC, the unit-cell radiation is represented by multipoles of order $|m| \neq 1$ [19], the radiations of which are intrinsically zero along **z** direction (see Figs. 1 and 3, and Ref. [19]) and can thus maintain the BIC on Γ point. In sharp contrast, for the accidental BICs shown in Fig. 4, zero radiation is accidental that originates from completely destructive multipolar interferences. Changing geometric parameters would alter the multipolar ratios and thus also the singularity positions, inevitably shifting the BICs. Moreover, as we have argued before, if the unit-cell radiation is represented by a dominant individual multipole, it is not possible to obtain positive index (topological charge) larger than +1 (see Table I), no matter which band we rely on. Though symmetry analysis reveals that large positive index is not forbidden [31,35–37], here we make a further step to show more microscopically that, to obtain a larger positive index, at least two combined multipoles are required (see Fig. 2). This is probably synonymous with the phenomenon that in previous studies large negative-index BIC have been widely achieved [31,35–37], whereas their positive counterparts rarely manifest themselves.

In conclusion, we revisit electromagnetic multipoles from a topological perspective and provide a comprehensive map for the distributions of singularities and their indices for multipolar radiations. It is shown that for an individual multipole, it is not possible to obtain singularity index larger than $+1$, while for the combination of a series of multipoles, there is no limit for its singularity, but only requires that index sum of all singularities over the momentum space has to be 2. Singularities of multipolar radiations are synonymous with the formation of BICs, as long as they coincide with open radiation channels. Based on this multipolar revelation, we further uncover the subtle equivalence between singularity indices of multipoles and topological charges of BICs. We emphasize here that by writing down Eqs. (1) and (4), we have confined our discussions to vector fields of pure real (or equivalently imaginary) nature. Nevertheless, electromagnetic waves are generally complex vector fields, from which we can define line fields (tensor fields) and thus line singularities and half-integer Hopf indices [10,11,38]. Such a study will be presented in our upcoming work. Considering the ubiquitous roles of electromagnetic multipoles all across photonics, our work will accelerate the pervasion of topological concepts into more optical branches and bring unperceived opportunities for various applications. Furthermore, multipoles basically serve as a fundamental tool and language for many other fields involving wave effects, on which our work generally sheds new light from a fundamental topological perspective.

We acknowledge the financial support from National Natural Science Foundation of China (Grants No. 11874026, No. 11404403, and No. 11874426) and the Outstanding Young Researcher Scheme of National University of Defense Technology. W. L. is grateful to Y. S. Kivshar and M. V. Berry for invaluable correspondences.

*yuntian@hust.edu.cn
†wei.liu.pku@gmail.com

[1] J. D. Jackson, *Classical Electrodynamics* (Wiley, New York, 1962).
[2] C. F. Bohren and D. R. Huffman, *Absorption and Scattering of Light by Small Particles* (Wiley, New York, 1983).
[3] R. E. Raab and O. L. de Lange, *Multipole Theory in Electromagnetism: Classical, Quantum, and Symmetry Aspects, With Applications* (Oxford University Press, Oxford, 2004).
[4] S. Jahani and Z. Jacob, All-dielectric metamaterials, Nat. Nanotechnol. **11**, 23 (2016).
[5] A. I. Kuznetsov, A. E. Miroshnichenko, M. L. Brongersma, Y. S. Kivshar, and B. Luk'yanchuk, Optically resonant dielectric nanostructures, Science **354**, aag2472 (2016).
[6] D. Smirnova and Y. S. Kivshar, Multipolar nonlinear nanophotonics, Optica **3**, 1241 (2016).
[7] W. Liu and Y. S. Kivshar, Generalized Kerker effects in nanophotonics and meta-optics [Invited], Opt. Express **26**, 13085 (2018).
[8] J. W. Milnor, *Topology from the Differentiable Viewpoint* (Princeton University Press, Princeton, NJ, 1997).
[9] D. S. Richeson, *Euler's Gem: The Polyhedron Formula and the Birth of Topology* (Princeton University Press, Princeton, NJ, 2012).
[10] G. J. Gbur, *Singular Optics* (CRC Press, Boca Raton, 2016).
[11] M. Berry, *Half-Century of Physical Asymptotics and Other Diversions: Selected Works by Michael Berry* (World Scientific, Singapore, Hackensack, NJ, 2017).
[12] M. Z. Hasan and C. L. Kane, Colloquium: Topological insulators, Rev. Mod. Phys. **82**, 3045 (2010).
[13] X.-L. Qi and S.-C. Zhang, Topological insulators and superconductors, Rev. Mod. Phys. **83**, 1057 (2011).
[14] Z. Yang, F. Gao, X. Shi, X. Lin, Z. Gao, Y. Chong, and B. Zhang, Topological Acoustics, Phys. Rev. Lett. **114**, 114301 (2015).
[15] S. D. Huber, Topological mechanics, Nat. Phys. **12**, 621 (2016).
[16] L. Lu, J. D. Joannopoulos, and M. Soljacic, Topological photonics, Nat. Photonics **8**, 821 (2014).
[17] T. Ozawa, H. M. Price, A. Amo, N. Goldman, M. Hafezi, L. Lu, M. C. Rechtsman, D. Schuster, J. Simon, O. Zilberberg, and I. Carusotto, Topological photonics, Rev. Mod. Phys. **91**, 015006 (2019).
[18] C. W. Hsu, B. Zhen, A. D. Stone, J. D. Joannopoulos, and M. Soljačić, Bound states in the continuum, Nat. Rev. Mater. **1**, 16048 (2016).
[19] See Supplemental Material at http://link.aps.org/supplemental/10.1103/PhysRevLett.122.153907 for sections (I) expressions for vector spherical harmonics, (II) positions and indices for singularities of the multipolar radiations, (III) radiation patterns, singularities, and indices for $\mathbf{M}^e_{lm}$ with $l = 1 \to 3$ and $m = 0 \to l$, (IV) multipolar expansions and the radiation patterns for unit cells of infinite periodic structures, (V) numerical calculations of the dispersion bands, the mode Q factors, and the field distributions within the unit cells of photonic crystal slabs, (VI) decay (non-BIC) states and separations of multipolar singularities from open radiation channels, (VII) multipolar compositions for the Γ-point BICs, and (VIII) off-Γ-point BICs of the hexagonal photonic crystal slab, which includes Refs. [20–22].
[20] W. Rudin, *Real and Complex Analysis*, 3rd ed. (McGraw-Hill Education, New York, 1986).
[21] A. Yariv and P. Yeh, *Photonics: Optical Electronics in Modern Communications* (Oxford University Press, Oxford, 2006).
[22] P. Grahn, A. Shevchenko, and M. Kaivola, Electromagnetic multipole theory for optical nanomaterials, New J. Phys. **14**, 093033 (2012).

[23] I. N. Bronshtein, K. A. Semendyayev, G. Musiol, and H. Mühlig, *Handbook of Mathematics*, 5th ed. (Springer, Berlin, New York, 2007).
[24] W. Liu, J. Zhang, B. Lei, H. Ma, W. Xie, and H. Hu, Ultra-directional forward scattering by individual core-shell nanoparticles, Opt. Express **22**, 16178 (2014).
[25] W. Liu, Generalized Magnetic Mirrors, Phys. Rev. Lett. **119**, 123902 (2017).
[26] T. Lepetit and B. Kanté, Controlling multipolar radiation with symmetries for electromagnetic bound states in the continuum, Phys. Rev. B **90**, 241103(R) (2014).
[27] F. Monticone and A. Alù, Bound states within the radiation continuum in diffraction gratings and the role of leaky modes, New J. Phys. **19**, 093011 (2017).
[28] W. Liu and A. E. Miroshnichenko, Beam steering with dielectric metalattices, ACS Photonics **5**, 1733 (2018).
[29] H. M. Doeleman, F. Monticone, W. den Hollander, A. Alù, and A. F. Koenderink, Experimental observation of a polarization vortex at an optical bound state in the continuum, Nat. Photonics **12**, 397 (2018).
[30] S. T. Ha, Y. H. Fu, N. K. Emani, Z. Pan, R. M. Bakker, R. Paniagua-Domínguez, and A. I. Kuznetsov, Directional lasing in resonant semiconductor nanoantenna arrays, Nat. Nanotechnol. **13**, 1042 (2018).
[31] B. Zhen, C. W. Hsu, L. Lu, A. D. Stone, and M. Soljačić, Topological Nature of Optical Bound States in the Continuum, Phys. Rev. Lett. **113**, 257401 (2014).
[32] Y. Yang, C. Peng, Y. Liang, Z. Li, and S. Noda, Analytical Perspective for Bound States in the Continuum in Photonic Crystal Slabs, Phys. Rev. Lett. **113**, 037401 (2014).
[33] C. W. Hsu, B. Zhen, J. Lee, S.-L. Chua, S. G. Johnson, J. D. Joannopoulos, and M. Soljačić, Observation of trapped light within the radiation continuum, Nature (London) **499**, 188 (2013).
[34] Y. Guo, M. Xiao, and S. Fan, Topologically Protected Complete Polarization Conversion, Phys. Rev. Lett. **119**, 167401 (2017).
[35] A. Kodigala, T. Lepetit, Q. Gu, B. Bahari, Y. Fainman, and B. Kanté, Lasing action from photonic bound states in continuum, Nature (London) **541**, 196 (2017).
[36] Y. Zhang, A. Chen, W. Liu, C. W. Hsu, B. Wang, F. Guan, X. Liu, L. Shi, L. Lu, and J. Zi, Observation of Polarization Vortices in Momentum Space, Phys. Rev. Lett. **120**, 186103 (2018).
[37] K. Sakoda, *Optical Properties of Photonic Crystals*, 2nd ed. (Springer, Berlin, New York, 2004).
[38] H. Hopf, *Differential Geometry in the Large: Seminar Lectures New York University, 1946 and Stanford University, 1956* (Springer, New York, 2003).